NORTHWESTERN UNIVERSITY
Department of Electrical Engineering and Computer Science

Lecture 9 - EECS 379

PROPERTIES OF FABRY-PEROT LASERS

Reading Assignment: YARIV - Sec. 6.5.

9.1 Output Frequency Tuning

In arriving at the output power expression (8.15), we assumed that there was a Fabry-Perot (FP) resonance at the peak of the gain curve. Because of this, the intensity within the resonator grew up at $\nu = \nu_0$, and hence, the output was of frequency ν_0. This assumption, however, is not necessary. For laser action to occur, one only requires that the FP resonance condition (8.8), i.e., the positive feedback condition, be satisfied at some frequency ν_m within the band of frequencies for which the unsaturated gain is larger than the threshold value. The gain and loss spectra at and above threshold when $\nu_m \neq \nu_0$ are illustrated in Figs. 9.1 and 9.2, respectively. In this case, the output power is of frequency ν_m [note the comment before Eq. (8.10)] and can be written as

$$P_{\nu_m}^{\text{out}} = AT\frac{I_s(\nu_m)}{2}\left(\frac{W_p}{W_t(\nu_m)} - 1\right). \tag{9.1}$$

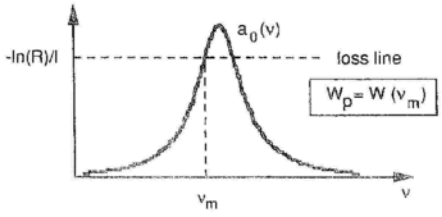

Figure 9.1: *Gain and loss spectra* at threshold *when* $\nu_m \neq \nu_0$.

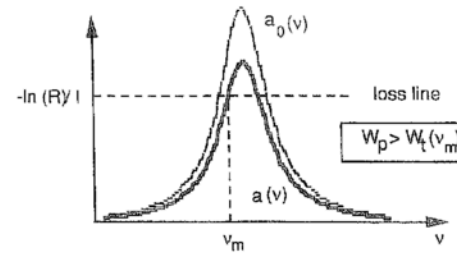

Figure 9.2: *Gain and loss spectra* above threshold *when* $\nu_m \neq \nu_0$.

where from Eqs. (7.30) and (8.12)

$$I_s(\nu_m) = \frac{8\pi h\nu_m}{\lambda^2 g(\nu_m)}. \tag{9.2}$$

$$W_t(\nu_m) = -\frac{8\pi \ln R}{\lambda^2 \ell N g(\nu_m)}. \tag{9.3}$$

Since both $I_s(\nu_m)$ and $W_t(\nu_m)$ are proportional to $1/g(\nu_m)$, the saturation intensity and the threshold pumping rate are higher at $\nu_m \neq \nu_0$ than those at $\nu_m = \nu_0$.

From Eqs. (8.9) and (8.10), we see that the resonance ν_m can be varied by changing the length ℓ of the Fabry-Perot (FP) cavity. One way to accomplish this is to mount one of the mirrors of the FP laser on a piezoelectric transducer (PZT). The thickness of a PZT can be controlled to within fractions of a micron by applying a voltage across it. Thus, the length of the laser cavity, and hence the resonance frequency, becomes proportional to the applied voltage. As ν_m varies, from Eqs. (9.1)-(9.3), the output power at ν_m also varies. At a given pumping rate, we obtain

$$\begin{aligned} P_{\nu_m}^{\text{out}} &= A\frac{T}{2}\frac{8\pi h\nu_m}{\lambda^2 g(\nu_m)}\left(-\frac{\lambda^2 \ell N g(\nu_m) W_p}{8\pi \ln R} - 1\right) \\ &= A\frac{T}{2}\left(-\frac{\ell N W_p h\nu_m}{\ln R} - \frac{8\pi h\nu_m}{\lambda^2 g(\nu_m)}\right) \\ &= A\frac{T}{2}\left(-\frac{\ell N W_p h\nu_m}{\ln R} - \frac{8\pi h\nu_m\left[(\nu_m-\nu_0)^2 + (\Delta\nu/2)^2\right]}{\lambda^2(\Delta\nu/2\pi)}\right) \end{aligned}$$

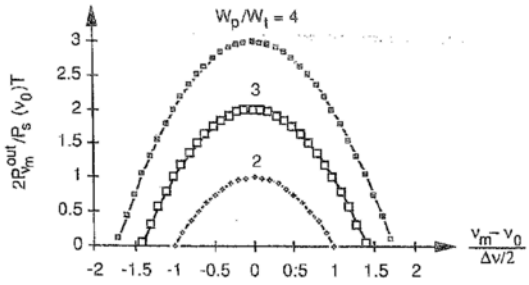

Figure 9.3: *Tuning range of an* FP *laser at* $W_p = 2W_t$, $3W_t$, *and* $4W_t$.

$$
\begin{aligned}
&= P^{\text{out}}_{\nu_0}\left[1 - \frac{\nu_m}{\nu_0}\frac{1}{W_p/W_t - 1}\left(\frac{\nu_m - \nu_0}{\Delta\nu/2}\right)^2\right] \\
&= \frac{P_s(\nu_0)T}{2}\left(\frac{W_p}{W_t} - 1\right)\left[1 - \frac{\nu_m}{\nu_0}\frac{1}{W_p/W_t - 1}\left(\frac{\nu_m - \nu_0}{\Delta\nu/2}\right)^2\right] \\
&\simeq \frac{P_s(\nu_0)T}{2}\left(\frac{W_p}{W_t} - 1\right)\left[1 - \frac{1}{W_p/W_t - 1}\left(\frac{\nu_m - \nu_0}{\Delta\nu/2}\right)^2\right]; \qquad (9.4)
\end{aligned}
$$

where in the third equality, we have substituted $g(\nu_m)$ from Eq. (5.23); in the fourth, used Eqs. (9.1)-(9.3); in the fifth, used Eq. (8.15); and when the ν dependence of W_t is not specified, it is assumed to be at $\nu = \nu_0$. The behavior of $P^{\text{out}}_{\nu_m}$ as a function of ν_m is plotted in Fig. 9.3. The tuning range Δ_T, i.e., the frequencies over which the laser can operate, is approximately given by

$$\Delta_T = \nu_0 \pm \frac{\Delta\nu}{2}\sqrt{\frac{W_p}{W_t(\nu_0)} - 1}. \qquad (9.5)$$

Thus, the range is wider at higher pumping rates. At $W_p = 2W_t$, for example, the FP laser is tunable over $\nu_0 \pm \Delta\nu/2$, a very limited range indeed for gases with $\Delta\nu \simeq 10^7$ Hz. In dye lasers $\Delta\nu$ can be larger than 10^{13} Hz giving a very large tunability range (wavelength tunability range in excess of 10 nm).

9.2 Internal Losses in an FP Laser

In derivation of Eq. (8.5), we assumed that the plane waves within the FP resonator do not experience any losses in propagation from one mirror to the other. In real lasers, however, this assumption is not quite valid. As we will learn in the second half of this course, at least there is loss due to diffraction. This results from the fact that the waves running back and forth within the FP resonator are not quite plane waves. In propagation from one mirror to the other, the cross-section of the electromagnetic wave increases due to diffraction, resulting in a part of the wave leaking out of the resonator.

The effect of internal losses within the laser can be included by generalizing the relation $R + T = 1$ to $R + T + L = 1$, where L is the fractional energy loss as the plane wave is reflected back and forth between the end mirrors of reflectivity R and transmitivity T. The lasing condition (8.6) then generalizes to

$$(1 - L - T)\exp\left[a(\nu)\ell + 2j\beta(\nu)\ell\right] = 1. \tag{9.6}$$

Taking the real and imaginary parts, we see that the FP resonance condition (8.8) stays intact whereas the energy conservation condition (8.7) modifies to

$$a(\nu) = -\frac{1}{\ell}\ln(1 - L - T). \tag{9.7}$$

In effect, in order for oscillation to occur, the round-trip fractional gain $\exp[a(\nu)\ell]$ must not only compensate for the round-trip fractional loss R at the mirrors, but also the internal round-trip fractional loss L. Following Eqs. (8.13)-(8.15) and Eqs. (9.1)-(9.3), the output power at ν_m is given by

$$P_{\nu_m}^{\text{out}} = \frac{AT}{2} I_s(\nu_m)\left[-\frac{a_0(\nu_m)\ell}{\ln(1 - L - T)} - 1\right]. \tag{9.8}$$

and the threshold pumping rate $W_t(\nu_m)$ gets modified to

$$W_t(\nu_m) = \frac{8\pi \ln(1 - L - T)}{\lambda^2 \ell N_2 g(\nu_m)}. \tag{9.9}$$

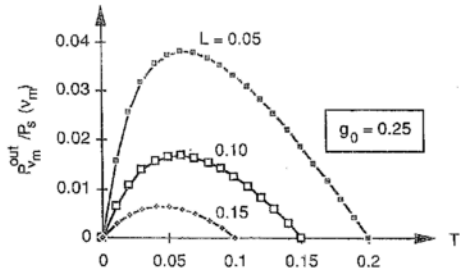

Figure 9.4: *Output power as function of T for various values of L.*

In typical lasers. He-Ne laser for example. $L + T \ll 1$. (Both L and T are about a few percent each.) Using the expansion $\ln(1+x) \simeq x$ for $x \ll 1$. Eqs. (9.8) and (9.9) simplify to

$$P^{\rm out}_{\nu_m} = \frac{TP_s(\nu_m)}{2}\left[\frac{a_0(\nu_m)\ell}{L+T} - 1\right]. \tag{9.10}$$

$$W_t(\nu_m) = \frac{8\pi(L+T)}{\lambda^2 \ell \mathcal{N} g(\nu_m)}. \tag{9.11}$$

where $P_s(\nu_m) = AI_s(\nu_m)$. We see that the threshold pumping rate $W_t(\nu_m)$ increases linearly with the internal loss L. Moreover. at a fixed pumping rate above threshold, i.e., $W_p > W_t(\nu_m)$. the output power $P^{\rm out}_{\nu_m}$ is inversely proportional to L. Thus. we conclude that the internal loss L must be minimized in order to obtain efficient laser action.

9.3 Optimum Output Coupling

From Eq. (9.10). it is clear that the output power $P^{\rm out}_{\nu_m}$ depends upon T in a complicated way. In many lasers $g_0 \equiv a_0(\nu_m)\ell$ is much less than one. typically ranging from a few percent to a few tens of percent. Therefore. $P^{\rm out}_{\nu_m}$ goes to zero at $T = 0$ and at $T = g_0 - L$. In between there is an optimum value at which the output power is maximized. This optimum value is of utmost importance in designing an efficient laser. In Fig. 9.4. we plot $P^{\rm out}_{\nu_m}/P_s(\nu_m)$ as a function of T for a given g_0 and for various values of L. We see that the optimum T value

T_{opt} and the optimum output power $P_{\nu_m}^{\text{opt}}$ depends upon L. To determine T_{opt} and $P_{\nu_m}^{\text{opt}}$, we set the derivative of Eq. (9.10) equal to zero. Substituting $g_0 = a_0(\nu_m)\ell$, we get

$$\begin{aligned}\frac{d}{dT}P_{\nu_m}^{\text{out}} &= \frac{d}{dT}\left[\frac{TP_s(\nu_m)}{2}\left(\frac{g_0}{L+T}-1\right)\right] \\ &= \frac{P_s(\nu_m)}{2}\left[\left(\frac{g_0}{L+T}-1\right)-T\frac{g_0}{(L+T)^2}\right] \\ &= 0. \end{aligned} \tag{9.12}$$

Solving for T and substituting back in Eq. (9.10), we get

$$T_{\text{opt}} = \sqrt{g_0 L} - L. \tag{9.13}$$

$$P_{\nu_m}^{\text{opt}} = \frac{P_s(\nu_m)}{2}\left(\sqrt{g_0}-\sqrt{L}\right)^2. \tag{9.14}$$

Thus, we see that the optimum output power, and the transmissivity of the mirrors required to obtain that, depends only upon the unsaturated single-pass gain $g_0 = a_0(\nu_m)\ell$ and the internal-loss factor L. Both g_0 and L must be known before an efficient Fabry-Perot laser can be designed.

NORTHWESTERN UNIVERSITY
Department of Electrical Engineering and Computer Science

Lecture 10 – EECS 379

HOMOGENEOUS AND INHOMOGENEOUS BROADENING

Reading Assignment: YARIV – Secs. 5.1 and 5.7.

10.1 Introduction

In the generic laser theory presented in the previous three lectures, we have implicitely assumed that all the atoms (or molecules) of the gain medium behave identically so far as the atom-field interaction is concerned. A gain medium in which all the atoms behave identically is referred to as *homogeneously broadened*. The term "broadened" signifies the fact that the gain occurs over a band of frequencies $\Delta\nu$, the homogeneous linewidth of the medium, around ν_0, as determined by the normalized lineshape function $g(\nu)$ of Eq. (5.23). Due to the homogeneity, the lasing modes of the Fabry-Perot (FP) resonator, separated by $c/2\ell$, interact simultaneously with all the atoms in the gain medium. It turns out then that only one mode of the FP resonator can oscillate at a time. The reason for this single mode operation is as follows: If there are more than one modes for which the unsaturated gain is above threshold, then initially they all start to oscillate. But, eventually in steady state, the one that sees the highest gain wins as it pulls the gain down, via gain saturation, for the remaining modes to a below-threshold level. In Fig. 10.1, we illustrate both the unsaturated and saturated gain spectra for the case in which there are three modes that see an above-threshold unsaturated gain.

Many of the laser media, however, are not homogeneously broadened. In such lasers multimode or multifrequency operation is possible. Gain media in which different groups of atoms interact differently with light of frequency ν are referred to as *inhomogeneously broadened*. The gas lasers (He-Ne, Ar^+, Kr^+, CO_2, etc.) and most of the solid state lasers

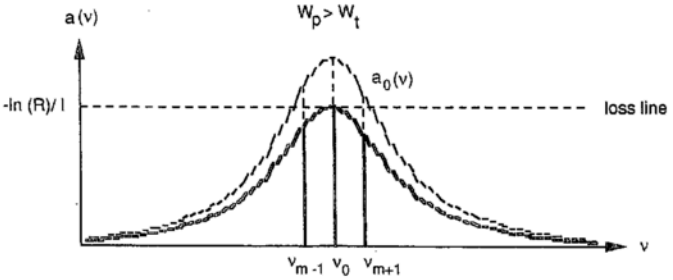

Figure 10.1: *Gain spectra that illustrate single-mode operation of homogeneously broadened lasers.*

(Nd:YAG, Ruby, etc.) fall into this category. In the former, the Doppler effect causes a shift in the resonance frequency of an active atom. The shift depends upon the speed at which the particular atom is moving. In the generic laser theory developed in the previous two lectures, we assumed all the participating atoms to be at rest. In solid-state lasers, on the other hand, the active atoms are embedded at fixed locations in a host crystal, e.g., Yttrium Aluminum Garnet (YAG) in the Nd:YAG laser. Atoms at different sites see different environments in the crystal due to imperfections in the crystal structure resulting from impurities, strains, dislocations, etc. The prevailing environment at a particular site causes a shift in the resonance frequency of the atom that varies from site to site.

In this and the following Lecture, we develop the generic theory of a laser that employs an inhomogeneously-broadened gain medium, in particular, a Doppler-broadened gain medium as in gas lasers.

10.2 Doppler Broadening

Consider an atom which is moving along the z direction with speed v_z as shown in Fig. 10.2. The resonance frequency of the atom in its rest frame is given by $\nu_0 = (Q_2 - Q_1)/h$. If a monochromatic plane wave of frequency ν is also propagating along the z direction, then

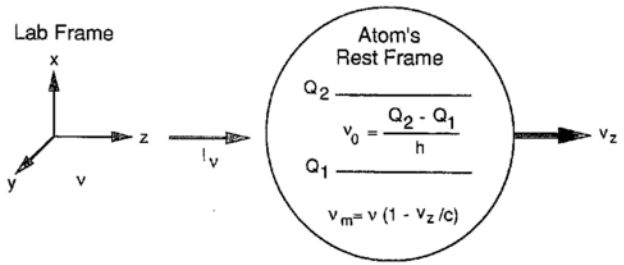

Figure 10.2: *Frequency ν appears as $\nu_M = \nu(1 - v_z/c)$ to a moving atom.*

in the rest frame of the atom, due to the Doppler effect, it appears to have a frequency $\nu_M = \nu(1 - v_z/c)$. Here, we consider only the first order Doppler effect, which is valid whenever $v_z/c \ll 1$. For gases at room temperature, v_z/c is certainly less than one. Thus, if $\nu = \nu_0$, i.e., if the light frequency is equal to the resonance frequency of the moving atom, then in the rest frame of the atom, the plane wave will not be resonant with the atom.

The strength of the interaction between an atom and the lightwave depends upon the normalized lineshape function $g(\nu)$ of Eq. (5.23). For a moving atom with v_z as the z component of its velocity, $g(\nu)$will be given by

$$\begin{aligned} g(\nu = \nu_M) &= \frac{\Delta\nu/2\pi}{(\nu_M - \nu_0)^2 + (\Delta\nu/2)^2} \\ &= \frac{\Delta\nu/2\pi}{(\nu - \nu v_z/c - \nu_0)^2 + (\Delta\nu/2)^2} \\ &\simeq \frac{\Delta\nu/2\pi}{[\nu - \nu_0(1 + v_z/c)]^2 + (\Delta\nu/2)^2}, \end{aligned} \tag{10.1}$$

where we have replaced $\nu v_z/c$ by $\nu_0 v_z/c$ in the last approximate equality. From the above expression, we see that in the lab frame, where the lightwave has frequency ν, it appears as if the atomic resonance frequency is shifted up from ν_0 to $\nu_0(1+v_z/c)$ so far as the atom-field interaction is concerned. We will emphasize this fact by writing $g(\nu_M)$ as $G\big(\nu : \nu_0(1+v_z/c)\big)$, where the implicit dependence on v_z is noted. Thus, if the atom's velocity component along

the plane wave is v_z, then its interaction with the latter in the lab frame is proportional to $G\big(\nu : \nu_0(1 + v_z/c)\big)$. In a gaseous medium, the plane wave will interact with all the constituent atoms (or molecules) having different values of v_z. In order to determine the total interaction strength, we must sum over the effect of all the atoms.

Let us assume that there are N atoms per unit volume in the medium. Then the number of atoms per unit volume with the z component of their velocities between v_z and $v_z + dv_z$ is given by $Nf(v_z)dv_z$, where $f(v_z)$ is the probability that an atom has the z component of its velocity between v_z and $v_z + dv_z$. $f(v_z)$ is given by the Maxwell-Boltzman distribution of atomic velocities in a gaseous medium. At temperature T, the Maxwell-Boltzman distribution can be written as

$$f(v_z) = \sqrt{\frac{M}{2\pi k_B T}} \exp\left(-\frac{M v_z^2}{2k_B T}\right), \tag{10.2}$$

where M is the mass of the constitutent atoms or molecules. In order to interpret it as a probability, the distribution is normalized such that

$$\int_{-\infty}^{\infty} f(v_z)dv_z = 1. \tag{10.3}$$

The interaction strength of the plane wave with all the constituent atoms of the medium will then be proportional to the following lineshape function:

$$g(\nu) = \int_{-\infty}^{\infty} dv_z f(v_z) G\big(\nu : \nu_0(1 + v_z/c)\big). \tag{10.4}$$

In Fig. 10.3, we have plotted the v_z dependence of $G\big(\nu : \nu_0(1 + v_z/c)\big)$ together with that of $f(v_z)$ for a typical gas. The v_z dependence of $G\big(\nu : \nu_0(1 + v_z/c)\big)$ can be seen by writing it as

$$\begin{aligned} G\big(\nu : \nu_0(1 + v_z/c)\big) &= \frac{\Delta\nu/2\pi}{[\nu - \nu_0(1 + v_z/c)]^2 + (\Delta\nu/2)^2} \\ &= \frac{c^2\Delta\nu/2\pi\nu_0^2}{[v_z - c(\nu - \nu_0)/\nu_0]^2 + (c\Delta\nu/2\nu_0)^2}. \end{aligned} \tag{10.5}$$

Thus, the v_z dependence of $G\big(\nu : \nu_0(1+v_z/c)\big)$ is centered at $v_{z0} = c(\nu-\nu_0)/\nu_0$ and has a full

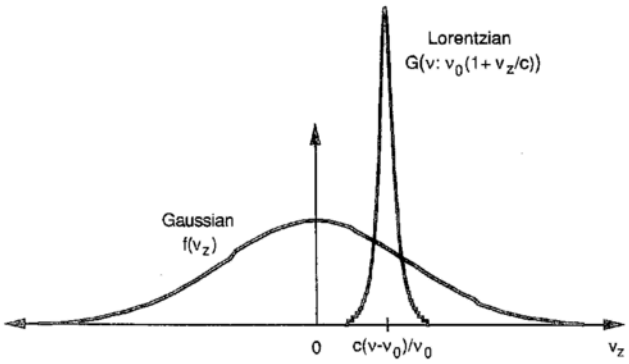

Figure 10.3: *Plots of* $G\big(\nu : \nu_0(1+v_z/c)\big)$ *and* $f(v_z)$ *as a function of* v_z.

width at half maximum (FWHM) of $c\Delta\nu/\nu_0$. For a typical gas, Ne for example, $\Delta\nu \simeq 10^7$ Hz and $\nu_0 \simeq 5 \times 10^{14}$ Hz implies a FWHM of the velocity distribution as $\simeq 6\,\mathrm{ms}^{-1}$. From Eq. (10.2), the FWHM of the Maxwell-Boltzman distribution is given by $2(2k_BT\ln 2/M)^{1/2}$, which for Ne atoms ($M = 1.67 \times 10^{-26}$ Kg) at room temperature ($T = 300$ K) $\simeq 1172\,\mathrm{ms}^{-1}$. Therefore, we see that, to a very good approximation, the width of $G\big(\nu : \nu_0(1+v_z/c)\big)$ is much smaller than that of $f(v_z)$. This allows us to approximate $G\big(\nu : \nu_0(1+v_z/c)\big)$ by $\delta\big(\nu - \nu_0(1+v_z/c)\big)$ in Eq. (10.4). We obtain

$$\begin{aligned} g(\nu) &= \int_{-\infty}^{\infty} dv_z f(v_z)\delta\big(\nu - \nu_0(1+v_z/c)\big) \\ &= \int_{-\infty}^{\infty} f(v_z)\delta\big(v_z - c(\nu-\nu_0)/\nu_0\big)\frac{c}{\nu_0}dv_z \\ &= \frac{c}{\nu_0} f\big(v_z = c(\nu-\nu_0)/\nu_0\big) \\ &\equiv g_D(\nu). \end{aligned} \tag{10.6}$$

where we have defined $g_D(\nu)$ to signify the above approximation. Using Eq. (10.2), $g_D(\nu)$

can also be written as

$$g_D(\nu) = \frac{c}{\nu_0}\sqrt{\frac{M}{2\pi k_B T}}\exp\left(-\frac{Mc^2(\nu-\nu_0)^2}{2\nu_0^2 k_B T}\right)$$

$$\equiv \sqrt{\frac{\ln 2}{\pi(\Delta\nu_D/2)^2}}\exp\left(-\frac{(\nu-\nu_0)^2}{(\Delta\nu_D/2)^2}\ln 2\right), \tag{10.7}$$

where we have defined the Doppler width or the Doppler-broadened linewidth $\Delta\nu_D$ as

$$\Delta\nu_D \equiv \frac{2\nu_0}{c}\sqrt{\frac{2k_B T}{M}\ln 2}. \tag{10.8}$$

NORTHWESTERN UNIVERSITY
Department of Electrical and Computer Engineering

ECE 379 - Lecture 11

MULTIMODE LASER OPERATION

Reading Assignment: YARIV - Secs. 5.7 and 6.6.

11.1 Population Inversion and Gain in a Doppler Broadened Medium

To see how Doppler broadening affects the gain in a laser, we re-examine the system of four-level atoms. Let us assume that the pumping rate W_p is independent of the velocity component v_z. Such would be the case, for example, in a gas-discharge laser where the excitation is due to collisions of the accelerating electrons with the four-level atoms. We first consider the case with $I_\nu = 0$, i.e., the case when there is no light present in system of four-level atoms.

If we concentrate on the group of atoms that have the z component of their velocities between v_z and $v_z + dv_z$, then from Eqs. (7.15) and (7.16), the contribution to the population inversion and the unsaturated gain by this group can be written as

$$\Delta N^0_{v_z} = N_{v_z} W_p t_{21}, \tag{11.1}$$

$$a_0^{v_z}(\nu) = \frac{\lambda^2 N_{v_z} W_p}{8\pi} G\Big(\nu : \nu_0(1 + v_z/c)\Big) \tag{11.2}$$

respectively, where $N_{v_z} = N f(v_z)$ is the number of atoms per unit volume in this group. The total unsaturated gain can be obtained by summing over the contributions of the various groups of atoms with different v_z values. The total unsaturated gain, therefore, is

$$\begin{aligned} a_0(\nu) &= \int_{-\infty}^{\infty} a_0^{v_z}(\nu) dv_z \\ &= \frac{\lambda^2 W_p N}{8\pi} \int_{-\infty}^{\infty} f(v_z) G\Big(\nu : \nu_0(1 + v_z/c)\Big)\, dv_z \\ &\simeq \frac{\lambda^2 N W_p}{8\pi} g_D(\nu), \end{aligned} \tag{11.3}$$

where in the last approximate equality we have used Eq. (10.6). Thus the only difference between the Doppler-broadened gain, Eq. (11.3), and the homogeneously-broadened gain, Eq. (7.16), is the appearance of the lineshape function $g_D(\nu)$ instead of $g(\nu)$. Since, at any frequency ν, $g_D(\nu) \ll g(\nu)$ [because, both $g_D(\nu)$ and $g(\nu)$ are normalized to unity and $\Delta\nu_D \gg \Delta\nu$], the gain available in a Doppler-broadened medium at a given pumping rate is much less than that available in a homogeneously-broadened medium. This is because in a Doppler-broadened medium, only a small fraction of the inverted atoms take part in providing the gain at a given frequency.

11.2 Gain Saturation in a Doppler Broadened Medium

Now we generalize to the case in which there is nonzero light intensity I_ν at frequency ν. Once again, considering only the group of atoms with the z component of their velocities between v_z and $v_z + dv_z$, from Eqs. (7.29) and (7.30), we have

$$a^{v_z}(\nu) = \frac{a_0^{v_z}(\nu)}{1 + I_\nu / I_s\Big(\nu : \nu_0(1 + v_z/c)\Big)}, \tag{11.4}$$

where

$$I_s\Big(\nu : \nu_0(1 + v_z/c)\Big) = \frac{8\pi h\nu}{\lambda^2 G\Big(\nu : \nu_0(1 + v_z/c)\Big)}. \tag{11.5}$$

Similar to Eq. (11.3), the total gain is obtained by adding the contributions of all the atoms. Integrating $a^{v_z}(\nu)$ over v_z, we obtain

$$\begin{aligned} a(\nu) &= \int_{-\infty}^{\infty} dv_z\, a^{v_z}(\nu) \\ &= \int_{-\infty}^{\infty} dv_z \frac{a_0^{v_z}(\nu)}{1 + I_\nu / I_s\Big(\nu : \nu_0(1 + v_z/c)\Big)} \\ &= \frac{\lambda^2 N W_p}{8\pi} \int_{-\infty}^{\infty} dv_z \frac{f(v_z) G\Big(\nu : \nu_0(1 + v_z/c)\Big)}{1 + \lambda^2 I_\nu G\Big(\nu : \nu_0(1 + v_z/c)\Big)/8\pi h\nu}, \end{aligned} \tag{11.6}$$

where in the second equality, we have substituted Eq. (11.4), and in the third, Eqs. (11.2) and (11.5). Using Eq. (10.5), the above integral can be cast in the following form:

$$a(\nu) = \frac{\lambda^2 W_p N}{8\pi} \int_{-\infty}^{\infty} dv_z \frac{f(v_z)}{(\lambda^2 I_\nu / 8\pi h\nu) + 1/G\Big(\nu : \nu_0(1 + v_z/c)\Big)}$$

$$= \frac{\lambda^2 N W_p}{8\pi}\frac{c^2\Delta\nu}{2\pi\nu_0^2}\int_{-\infty}^{\infty} dv_z \times \frac{f(v_z)}{\Big(v_z - c(\nu-\nu_0)/\nu_0\Big)^2 + \Big[c^2\big((\Delta\nu/2)^2 + (\Delta\nu/2\pi)(\lambda^2 I_\nu/8\pi h\nu)\big)/\nu_0^2\Big]}. \tag{11.7}$$

The integrand is a product of two functions, a Gaussian $f(v_z)$ [cf. Eq. (10.2)] and a Lorentzian similar to $G\big(\nu : \nu_0(1+v_z/c)\big)$ of Eq. (10.5). In typical circumstances, the width of the Lorentzian is much narrower than the width of the Gaussian. We have already noted this in arriving at Eq. (10.6). Therefore, we can approximate Eq. (11.7) by evaluating $f(v_z)$ at the peak of the Lorentzian at $v_z = c(\nu-\nu_0)/\nu_0$, and pulling it out of the integral. The remaining integral is of the form $\int_{-\infty}^{\infty} dx/(x^2+a^2)$ with $a = \frac{c}{\nu_0}\Big[(\frac{\Delta\nu}{2})^2 + \frac{\Delta\nu}{2\pi}\frac{\lambda^2 I_\nu}{8\pi h\nu}\Big]^{1/2}$, and is equal to π/a. Carrying out the above steps, we get

$$\begin{aligned} a(\nu) &\simeq \frac{\lambda^2 N W_p}{8\pi}\frac{c^2\Delta\nu}{2\pi\nu_0^2} f\big(v_z = (\nu-\nu_0)c/\nu_0\big) \\ &\quad \times \int_{-\infty}^{\infty} dv_z \frac{1}{\Big(v_z - c(\nu-\nu_0)/\nu_0\Big)^2 + \Big[c^2\big((\Delta\nu/2)^2 + (\Delta\nu/2\pi)(\lambda^2 I_\nu/8\pi h\nu)\big)/\nu_0^2\Big]} \\ &= \frac{\lambda^2 N W_p}{8\pi}\frac{c^2\Delta\nu}{2\pi\nu_0^2} f\big(v_z = c(\nu-\nu_0)/\nu_0\big) \\ &\quad \times \frac{\pi}{(c/\nu_0)\Big[(\Delta\nu/2)^2 + (\Delta\nu/2\pi)(\lambda^2 I_\nu/8\pi h\nu)\Big]^{1/2}}, \end{aligned} \tag{11.8}$$

which using Eqs. (10.6) and (11.3) further simplifies to the following expression for the saturated gain

$$\begin{aligned} a(\nu) &= \frac{\lambda^2 N W_p}{8\pi} g_D(\nu)\frac{\Delta\nu}{2}\frac{1}{\Big[(\Delta\nu/2)^2 + (\Delta\nu/2\pi)(\lambda^2 I_\nu/8\pi h\nu)\Big]^{1/2}} \\ &= \frac{a_0(\nu)}{\Big(1 + \lambda^2 I_\nu/4\pi^2 h\nu\Delta\nu\Big)^{1/2}} \\ &\equiv \frac{a_0(\nu)}{\sqrt{1 + I_\nu/I_s^D}}. \end{aligned} \tag{11.9}$$

In the last equality, we have defined the saturation intensity for a Doppler broadened medium by

$$I_s^D \equiv \frac{4\pi^2 h\nu\Delta\nu}{\lambda^2}, \tag{11.10}$$

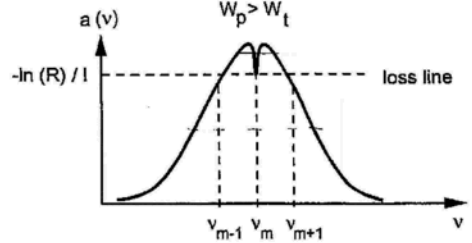

Figure 11.1: *Gain and loss spectra for single-mode operation.*

which is a very mild function of frequency, unlike the homogeneously-broadened medium case. In fact, comparing with Eq. (7.30), we find that $I_s^D = \nu I_s(\nu_0)/\nu_0$.

11.3 Laser Action with Doppler Broadened Gain

We pointed out in the introduction to the previous lecture that it is possible to obtain multimode operation in a laser with an inhomogeneously broadened gain. Before considering the general multimode case, let us assume that the pump parameter W_p is small so that only one mode of the Fabry-Perot resonator is above threshold.

11.3.1 Single Mode Operation

If the mode with frequency ν_m sees an unsaturated gain that is above threshold, then, in steady state, I_{ν_m} will grow to a value for which the *saturated* round-trip fractional gain equals the round-trip fractional loss, as illustrated in Fig. 11.1. (See Sec. 8.4 for the homogeneously broadened laser case.) From Eq. (11.9), the steady state I_{ν_m} is governed by

$$a(\nu_m) = \frac{a_0(\nu_m)}{\sqrt{1 + I_{\nu_m}/I_s^D}} = -\frac{1}{\ell} \ln R. \tag{11.11}$$

The threshold pumping rate for oscillation of the mode at ν_m is determined by

$$a_0(\nu_m) = \frac{\lambda^2 N W_t}{8\pi} g_D(\nu_m) = -\frac{1}{\ell} \ln R, \tag{11.12}$$

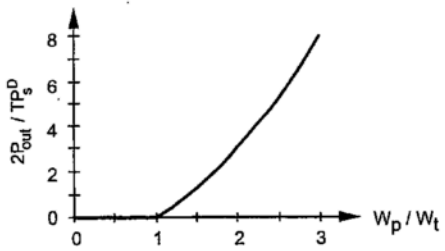

Figure 11.2: *Output power versus the pumping rate for an inhomogeneously-broadened single-mode laser.*

where we have used Eq. (11.3). The above equation when solved yields

$$W_t(\nu_m) = -\frac{8\pi \ln R}{\lambda^2 \ell N g_D(\nu_m)}. \tag{11.13}$$

Above threshold, i.e., at a pumping rate $W_p > W_t$, solving Eq. (11.11) leads to the following expression for the light intensity within the FP resonator containing the inhomogeneously-broadened gain medium:

$$\begin{aligned} I_{\nu_m} &= I_s^D \left[\left(\frac{a_0(\nu_m)}{-\frac{1}{\ell} \ln R} \right)^2 - 1 \right] \\ &= I_s^D \left[\left(\frac{W_p}{W_t} \right)^2 - 1 \right]. \end{aligned} \tag{11.14}$$

As in Sec. 8.4, the output power is given by

$$P_{\nu_m}^{\text{out}} = \frac{T}{2} P_s^D \left[\left(\frac{W_p}{W_t} \right)^2 - 1 \right], \tag{11.15}$$

where $P_s^D = A I_s^D$ is the intracavity saturation power. In Fig. 11.2, we plot the output power as a function of W_p/W_t. In contrast to the homogeneously-broadened laser case, the output power is a quadratic function of W_p/W_t.

11.3.2 Multimode Operation

It is clear from Eq. (11.4) that, for above threshold pumping, the saturated gain, as given by Eq. (11.9), is clamped at the loss line only within a narrow frequency region of approximate

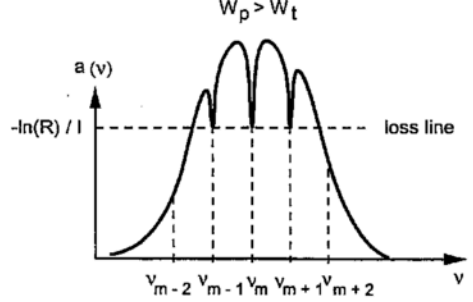

Figure 11.3: *Gain and loss spectra for multimode operation.*

width $\Delta\nu$ around ν_m. This is because I_{ν_m}, the intensity at ν_m that builds up within the FP resonator as a result of the laser action, saturates only that group of atoms which is resonant with ν_m. Atoms belonging to other groups get Doppler shifted out of resonance with ν_m, and are not affected at all. These atoms are available for providing gain at frequencies that lie outside the $\nu_m \pm \Delta\nu$ region. Because of our assumption that the pumping rate W_p be independent of frequency, we see from Eq. (11.3) that there is a wide frequency range over which gain exceeds loss in the presence of light at frequency ν_m. This behavior is graphically illustrated in Fig. 11.1. If there are modes of the FP resonator [i.e., frequencies at which the positive feedback condition (8.8) is satisfied] that lie in the frequency band where gain exceeds loss, oscillation will build up at these frequencies resulting in multimode operation of the laser. This situation is depicted graphically in Fig. 11.3. In a typical gas laser $\Delta\nu_D > c/2\ell \gg \Delta\nu$, and multimode operation occurs very frequently. In the He-Ne laser that you have seen in the laboratory, ℓ is typically 15 cm, $\Delta\nu \simeq 10$ MHz, and $\Delta\nu_D \simeq 3$ GHz. Therefore, the FP modes are $c/2\ell = 1$ GHz apart. This results in simultaneous oscillation of two or three frequencies in the laser.

The intensity in each of the lasing modes follows Eq. (11.14) with W_t depending upon ν_m via Eq. (11.13). The output power is given by Eq. (11.15) which can be rewritten as

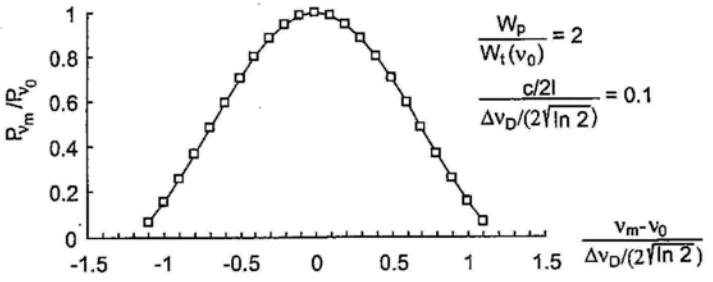

Figure 11.4: *Relative output power of the various lasing frequencies under multimode operation of a Doppler-broadened laser.*

$$P^{\text{out}}_{\nu_m} = P_{\nu_0}\left[\frac{\left(W_p/W_t(\nu_o)\right)^2 \exp\left[-2(\nu_m-\nu_0)^2/(\Delta\nu_D/2\sqrt{\ln 2})^2\right]-1}{\left(W_p/W_t(\nu_o)\right)^2-1}\right], \tag{11.16}$$

where $W_t(\nu_o)$ is the threshold pumping rate at the Doppler-broadened line center, and P_{ν_0} is the output power at ν_0 for a pumping rate of W_p. In Fig. 11.4, we plot the relative output power of the various lasing modes for the case where $W_p/W_t(\nu_0) = 2$ and $2\sqrt{\ln 2}(c/2l)/\Delta\nu_D = 0.1$. For these parameters, 23 longitudinal modes of the FP resonator oscillate simultaneously.

In the next lecture, we will see how the light at these various frequencies can be phase-locked to obtain ultrashort pulses of light.

This papge intentionally left blank.

NORTHWESTERN UNIVERSITY
Department of Electrical Engineering and Computer Science

Lecture 12 - EECS 379

MODE LOCKING

Reading Assignment: YARIV - Sec. 6.6 and 6.7

12.1 Incoherent Nature of the Multimode Output

We saw in the previous lecture that a Doppler-broadened laser can oscillate simultaneously in many longitudinal modes. The number M of the lasing modes is determined by how far above threshold the laser is pumped (cf. Eq. 11.16). Let us assume that all these modes are linearly polarized along the same direction. This can be accomplished, for example, by introducing Brewster windows in the laser cavity. (A TM mode sees less loss upon reflection from a Brewster window than a TE mode. Therefore, when a mode at frequency ν_m goes above threshold, both TE and TM modes compete for the same gain with the latter suppressing the former because of its lower loss.) The time dependence of the real electric field for the mth longitudinal plane-wave mode can be written as

$$e_m(t) = \mathrm{Re}\left[(2I_m/\epsilon_0 c)^{1/2}\exp[-j(\omega_0 + m\omega)t + j\phi_m]\right], \tag{12.1}$$

where $\omega = \pi c/\ell$ is the longitudinal mode spacing, and I_m is the intensity of the mth mode. In general, the phase ϕ_m of a given mode is randomly determined and has no relationship with the phases of the other lasing modes. The total electric field due to all the M modes is then

$$e(t) = \mathrm{Re}\left[\sum_{m=-\frac{M-1}{2}}^{\frac{M-1}{2}} (2I_0/\epsilon_0 c)^{1/2}\exp[-j(\omega_0 + m\omega) + j\phi_m]\right]. \tag{12.2}$$

In Fig. 12.1, we plot the time dependence of the total output intensity $I(t)$ of a laser that oscillates simultaneously in 11 longitudinal modes. The random nature of the ϕ_m's causes $I(t)$ to fluctuate over time scales much shorter than the cavity round-trip time. If the ϕ_m's

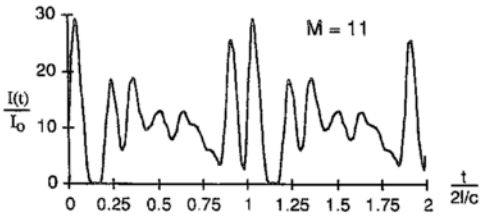

Figure 12.1: *Output intensity of a laser that oscillates simultaneously in 11 longitudinal modes with random phases.*

are also varying in time as is the case in most lasers, this results in temporal *in*coherence of the laser. In order to make the laser temporally coherent, one can do one of the following to ensure that only one longitudinal mode oscillates:

i) Operate the laser slightly above threshold so that only one mode sees gain higher than the loss.

ii) Shorten the cavity length so that only one longitudinal mode can be in the frequency region where gain exceeds loss.

iii) Introduce a tuning element in the cavity to modify the loss in a frequency selective way. All modes except for one, in the region where gain exceeds loss in the absence of the tuning element, see a loss that is higher than the gain with the tuning element present.

Since all of the above options decrease the number of lasing modes to only one, the total output power of the laser is drastically reduced. Both the total output power and the temporal coherence time can be increased by phase locking the various longitudinal modes as discussed in the next section.

12.2 Mode Locking

In this section, we show how the many longitudinal modes of a multimode laser can lead to the generation of short optical pulses. For simplicity, we assume that M is odd. Furthermore,

we assume that all of the m modes oscillate with the same intensity I_0, i.e., $I_m = I_0$ for all m. Later on we will point out the consequence if such an assumption is not made.

Mode locking occurs when the phases of all the oscillating modes are the same, i.e., $\phi_m = \phi_0$ for all m. In Sec. 12.4, we will see how such a condition can be achieved in practice. First, let us study the effects of mode locking. Substituting $\phi_m = \phi_0$ in Eq. (12.2), we get

$$\begin{aligned} e(t) &= \mathrm{Re}\left[(2I_0/\epsilon_0 c)^{1/2}\left(\sum_{-\frac{M-1}{2}}^{\frac{M-1}{2}} \exp(-jm\omega t)\right)\exp[-j(\omega_0 t - \phi_0)]\right] \\ &= \mathrm{Re}\left[(2I_0/\epsilon_0 c)^{1/2}\exp[j(M-1)\omega t/2]\frac{1-\exp(-jM\omega t)}{1-\exp(-j\omega t)}\exp[-j(\omega_0 t - \phi_0)]\right] \\ &= \mathrm{Re}\left[(2I_0/\epsilon_0 c)^{1/2}\frac{\sin(M\omega t/2)}{\sin(\omega t/2)}\exp[-j(\omega_0 t - \phi_0)]\right] \\ &= \mathcal{E}(t)\cos(\omega_0 t - \phi_0), \end{aligned} \tag{12.3}$$

where we have defined the time-domain pulse envelope $\mathcal{E}(t)$ via

$$\begin{aligned} \mathcal{E}(t) &\equiv (2I_0/\epsilon_0 c)^{1/2}\frac{\sin(M\omega t/2)}{\sin(\omega t/2)} \\ &= (2I_0/\epsilon_0 c)^{1/2} M \frac{\mathrm{sinc}(Mct/2\ell)}{\mathrm{sinc}(ct/2\ell)}, \end{aligned} \tag{12.4}$$

and $\mathrm{sinc}(x) \equiv \sin(\pi x)/(\pi x)$. The total intensity is given by

$$I(t) = M^2 I_0 \frac{\mathrm{sinc}^2(Mct/2\ell)}{\mathrm{sinc}^2(ct/2\ell)}. \tag{12.5}$$

Here, we point out that Eqs. (12.4) and (12.5) remain unchanged if M is not supposed to be odd.

12.3 Pulse Width, Pulse Height, and Average Intensity

We have plotted $I(t)$ vs. time in Fig. 12.2. It is a periodic function of time with period T determined via $cT/2\ell = 1$ or $T = 2\ell/c$, which is nothing but the round-trip time of the laser cavity. The nth maxima of $I(t)$ occur at $t_n = 2n\ell/c$ and the peak intensity is given by

$$I_{\mathrm{pk}} = I(t_n) = M^2 I_0. \tag{12.6}$$